

# Surrogate neutron-capture studies with fission detection in inverse kinematics at the ESR storage ring

Bogusław Włoch<sup>a</sup>, Camille Berthelot<sup>a</sup>, Guy Leckenby<sup>a</sup>, Beatriz Jurado<sup>a</sup>, Jerome Pibernat<sup>a</sup>, Manfred Grieser<sup>b</sup>, Jan Glorius<sup>c</sup>, Yuri Litvinov<sup>c</sup>, Laurent Audouin<sup>d</sup>, Bertram Blank<sup>a</sup>, Klaus Blaum<sup>b</sup>, Lucas Bégué–Guillou<sup>e</sup>, Alex Cobo Zarzuelo<sup>e</sup>, Sophia Florence Dellmann<sup>f</sup>, Marc Dupuis<sup>g,h</sup>, Oliver Forstner<sup>i</sup>, Alexis Francheteau<sup>e</sup>, David Freire Fernández<sup>j</sup>, Miki Fukutome<sup>k</sup>, Mathias Gerbaux<sup>a</sup>, Jérôme Giovannazzo<sup>a</sup>, Alexandre Gumberidze<sup>c</sup>, Andreas Heinz<sup>m</sup>, Ana Henriques<sup>n</sup>, Regina Hess<sup>c</sup>, Indu Jangid<sup>e</sup>, Anton Kalinin<sup>c</sup>, Wolfram Korten<sup>d</sup>, Sergey Litvinov<sup>c</sup>, Bernd Lorentz<sup>c</sup>, Antonio Moro<sup>p</sup>, Nikolaos Petridis<sup>c</sup>, Ulrich Popp<sup>c</sup>, Gregory Pote<sup>l</sup>, Diego Ramos<sup>e</sup>, Mathieu Roche<sup>a</sup>, Mohammad Shahab Sanjari<sup>c</sup>, Michele Sguazzin<sup>l</sup>, Ragandeep Singh Sidhu<sup>q</sup>, Uwe Spillmann<sup>c</sup>, Markus Steck<sup>c</sup>, Thomas Stoehlker<sup>i</sup>, Takayuki Yamaguchi<sup>r</sup>

<sup>a</sup>Université de Bordeaux, CNRS, LP2I Bordeaux, Gradignan, 33170, France

<sup>b</sup>Max-Planck-Institut für Kernphysik, Heidelberg, 69117, Germany

<sup>c</sup>GSI Helmholtzzentrum für Schwerionenforschung, Darmstadt, 64291, Germany

<sup>d</sup>CEA Paris-Saclay - DRF/IRFU/DPhN, Gif-sur-Yvette, 91191, France

<sup>e</sup>GANIL, CRNS/IN2P3-CEA/DRF, Caen, 14000, France

<sup>f</sup>Goethe Universität Frankfurt, Frankfurt am Main, 60438, Germany

<sup>g</sup>Commissariat à l'énergie atomique et aux énergies alternatives, DAM, DIF, Arpajon, 91297, France

<sup>h</sup>Université Paris-Saclay, LMCE, Bruyères-Le-Châtel, 91680, France

<sup>i</sup>Friedrich-Schiller-Universität Jena, Jena, 07743, Germany

<sup>j</sup>Universität zu Köln, Cologne, 50923, Germany

<sup>k</sup>Osaka University, Osaka, 565-0871, Japan

<sup>l</sup>Université Paris-Saclay, CNRS, IJCLab, Orsay, 91405, France

<sup>m</sup>Chalmers University of Technology, Gothenburg, 41296, Sweden

<sup>n</sup>Facility for Rare Isotope Beams, Michigan State University, East Lansing, 48824-1321, United States

<sup>o</sup>FH Aachen University of Applied Sciences, Aachen, 52066, Germany

<sup>p</sup>Universidad de Sevilla, Sevilla, 41004, Spain

<sup>q</sup>University of Surrey, Guildford, GU2 7XH, United Kingdom

<sup>r</sup>University of Saitama, Saitama, 338-8570, Japan

## Abstract

The NECTAR (Nuclear rEaCTions At storage Rings) experiment at the ESR heavy-ion storage ring at GSI Darmstadt is dedicated to surrogate reaction studies of neutron-induced reactions on heavy nuclei in inverse kinematics. In this work, we report on the implementation and performance of a newly developed fission-fragment detection system integrated into the NECTAR experimental setup. The upgraded detector configuration enables, for the first time in a surrogate experiment, the simultaneous detection of  $\gamma$ -decay residues, multi-neutron-emission residues, and fission fragments. The full setup was used for the first time in an experiment where a stored beam of bare  $^{238}\text{U}^{92+}$  ions at 17.24 MeV/u interacted with a gaseous deuterium target, populating excited  $^{238}\text{U}$  and  $^{239}\text{U}$  nuclei via the  $^{238}\text{U}(d,d')$  and  $^{238}\text{U}(d,p)$  reactions. We describe the fission detector geometry, design constraints, and simulation-based efficiency determination. The target-like particle identification and beam-like residue spectra demonstrating the performance of the complete setup are also shown.

**Keywords:** NECTAR, fission fragment detectors, surrogate reactions, heavy-ion storage rings, inverse kinematics

## 1. Introduction

Surrogate reaction techniques provide a powerful alternative for determining neutron-induced reaction cross sections of nuclei for which direct measurements are impractical, in particular short-lived or highly radioactive nuclei. In these methods, the same compound nucleus as formed in a neutron-induced reaction is populated through an alternative reaction mechanism, and its decay probabilities are measured as a function of excitation energy. By determining these decay probabilities, fundamental nuclear properties such as the nuclear level density (NLD), fission barrier heights, and the  $\gamma$ -strength function

( $\gamma$ SF) can be constrained [1, 2]. These quantities serve as critical inputs to reaction models and enable more reliable calculations of neutron-capture cross sections. Surrogate reactions are typically performed in direct kinematics. Decay probabilities are inferred from the detection of emitted  $\gamma$  rays or fission fragments using detector arrays surrounding the target [3, 4]. Although these approaches have been successfully applied, they often require substantial efficiency corrections and background subtraction.

The NECTAR (Nuclear rEaCTions At storage Rings) experimental program exploits the unique capabilities of heavy-ion storage rings to perform surrogate reaction measurements in-



Three fission detectors were installed in dedicated pockets mounted in fittings of the target chamber: two identical detectors positioned above and below the beam axis, and a third detector mounted on the horizontal plane on the outside of the ring. Together, these detectors provide large solid-angle coverage for forward-focused fission fragments.

The bottom, top, and side pockets were located at distances of 220 mm, 400 mm, and 340 mm from the target center, respectively. Due to geometrical constraints imposed by the chamber fittings, the side detector required a distinct mechanical design. A three-dimensional visualization of the chamber and pocket arrangement is shown in Fig. 3.

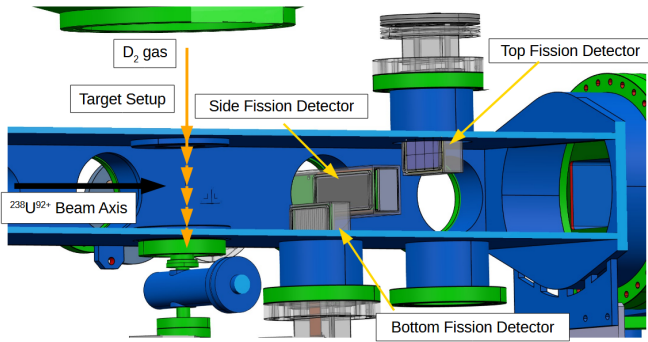


Figure 3: Cross section of the 3D model of the experimental chamber showing the integration of the fission detectors. The target-like detector (not visible) would be on the side of the viewer.

To prevent detector damage during beam injection, the side fission pocket was mounted on a movable system allowing it to be fully retracted during injection and inserted close to the beam axis only during data taking. The motion was achieved using a bellows system that preserved ultra-high vacuum conditions.

The top and bottom fission detectors were custom-designed BB36 DSSSDs from Micron Semiconductor Ltd., each with an active area of  $80 \times 40 \text{ mm}^2$  with a thickness of  $500 \mu\text{m}$  and a segmentation of 16 vertical by 16 horizontal strips. They were operated at a bias voltage of 100 V.

The side fission detector was a BB29 DSSSD with a thickness of  $500 \mu\text{m}$  and an active area of  $122 \times 40 \text{ mm}^2$ , segmented into 122 vertical and 40 horizontal strips. This detector design had previously been employed as the beam-like residue detector in the 2022 NECTAR experiment, facilitating reuse of existing electronics and mechanical components.

The fission detection system was studied using Monte Carlo simulations based on  $G4_{\text{BEAMLINE}}$  and the GEF code [7]. While fission fragments are emitted in all directions in the center-of-mass frame, the high beam velocity leads to strong forward focusing in the laboratory frame. For both  $^{238}\text{U}$  and  $^{239}\text{U}$  fissioning systems, the fragments are confined within a cone of approximately  $17^\circ$  around the beam axis.

The fission fragments kinetic energies in the laboratory frame vary between 9 MeV/u and 29 MeV/u, and practically do not depend on the excitation energy of the nucleus. At these energies, all the fragments went through the stainless-steel pocket windows and could reach the detectors with sufficient energy to ensure 100% intrinsic detection efficiency.

The full geometry of the reaction chamber, fission pockets, and detectors was implemented in the simulations. Figure 4 compares simulated and measured amplitude and hit distributions on the side fission detector. The clearly visible two-ring pattern comes from the detection of a light and a heavy fission fragment originating from the asymmetric fission mode of  $^{239}\text{U}$ , showing excellent agreement and validating the implemented geometry. The resulting fission detection efficiency was determined to be about 64% .

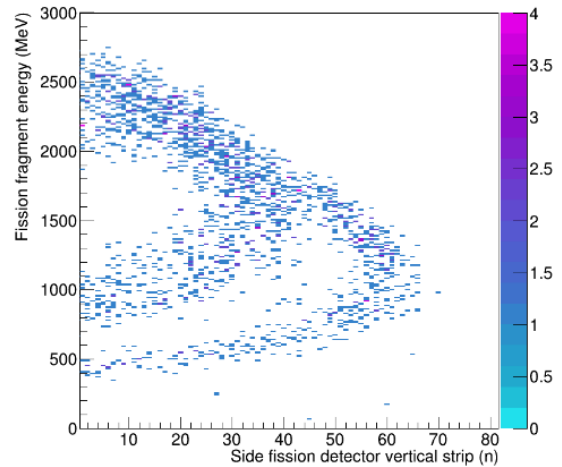
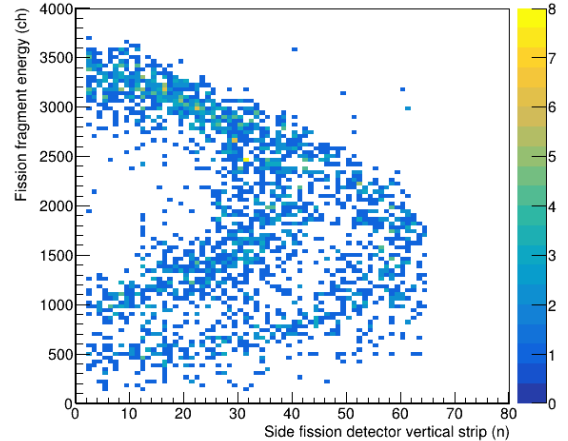


Figure 4: Comparison of measured (top) and simulated (bottom) fission-fragment hit distributions on the side detector. The energy of the fragments is represented as a function of their horizontal position measured with the vertical strips of the detector.

### 2.3. Beam-like residue detector

Different beam-like residues were separated using the ESR dipole magnet based on the difference in their magnetic rigidity and detected in a straight section of the ring. The detector employed the same BB29 DSSSD model design as the side fission detector, with minor differences in the mechanical supports.

The intrinsic efficiency of the detector was 100% for all residues reaching the detection plane. For the  $^{238}\text{U}(d,p)$  reaction, the Monte Carlo simulations showed full transmission of beam-like residues for  $\gamma$ -emission, one-neutron-emission and

two-neutron-emission. This implies an efficiency for determining  $\gamma$ , neutron and two-neutron emission probabilities of 100%, demonstrating the unique capabilities of NECTAR. The transmission for three-neutron-emission was below 100% because some of the heavy residues trajectories hit the wall of the ring beam pipe. The beam-like residues produced after four-neutron-emission were deflected too much inside the ring and none of them was able to reach the beam-like residue detector.

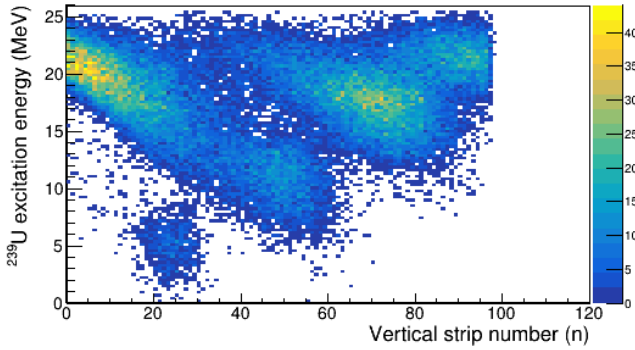


Figure 5: Beam-like detector identification spectra. The horizontal axis represents the horizontal position of beam-like residues after  $^{238}\text{U}(d,p)$  reaction. The vertical axis is the excitation energy of the compound nucleus.

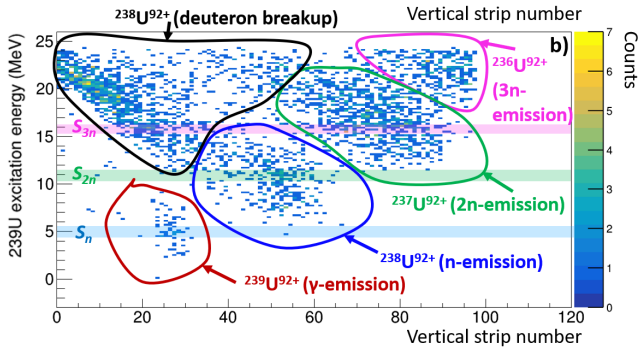


Figure 6: Similar as in Figure 5 but in coincidence with a proton detected in the 6th vertical strip of the target-like telescope detector. The marked areas indicate the different uranium isotopes and thus the different decay channels of the compound nucleus.

### 3. Beam-like residue identification spectra

The different decay channels of the compound nucleus formed in the  $^{238}\text{U}(d,p)$  reaction can be identified when plotting the vertical strip (horizontal position) of a hit in the beam-like detector versus the excitation energy of compound nucleus (Figure 5). The strips are numbered sequentially from zero to 122, with zero denoting the strip closest to the beam axis.

Different uranium isotopes form distinct bands that move closer to the edge of the detector as the nucleus excitation energy increases. The structures corresponding to the different decays are clearly visible, but there is also a relatively large amount of mixing between them. Therefore, to improve separation, we decided to repeat this procedure separately for each target-like telescope vertical strip. This narrows the angular

width of the detected target-like particles, thereby also reducing the spread of the peaks detected in the beam-like detector, as shown in Figure 6.

Below approximately 5 MeV, only  $\gamma$ -decay residues are observed. Above the neutron separation energy, distinct structures corresponding to one-, two-, and three-neutron emission appear at the expected thresholds.

At the highest excitation energies, a pronounced structure associated with heavy residues produced after deuteron breakup is observed. It is located closer to the beam axis, at strip numbers lower than 60. The ability to identify events originating from the deuteron breakup is a truly unique feature of the NECTAR experiment, as this has been impossible in all previous surrogate experiments with deuteron target in direct kinematics. This will allow with the further analysis of this experiment to use these events to subtract breakup contribution from the compound nucleus decay probabilities.

### 4. Conclusions

A dedicated fission-fragment detection system has been successfully designed, implemented, and commissioned for the NECTAR experiment at the ESR storage ring. The upgraded setup enables, for the first time, the simultaneous measurement of  $\gamma$ -decay, multi neutron-emission, and fission channels in a storage-ring based surrogate reaction experiment. The detector performance and efficiency have been validated through Monte-Carlo simulations and comparison with experimental data. Target-like and beam-like residues identification spectra showed the possibility of identifying all available decay channels. This development represents a crucial step toward complete surrogate measurements of neutron-induced reactions on heavy nuclei in inverse kinematics.

### Acknowledgments

This work is supported by the European Research Council (ERC) under the European Union's Horizon 2020 research and innovation programme (ERC-Advanced grant NECTAR, grant agreement No 884715). The results presented here are based on the experiment G-22-00028, which was performed at the ESR storage ring of the GSI Helmholtzzentrum fuer Schwerionenforschung, Darmstadt (Germany) in the context of FAIR Phase-0. We warmly thank the financial support from the GSI/IN2P3 collaboration 19-80. This project has also received funding from the European Union's Horizon Europe Research and Innovation programme under Grant Agreement No 101057511 (EURO-LABS).

### References

- [1] J. D. Cramer and H. C. Britt, Nucl. Sci. Eng. 41, 177 (1970).
- [2] J. E. Escher et al., Rev. Mod. Phys. 84, 353 (2012).

- [3] R. Perez Sanchez et al., Phys. Rev. Lett. 125, 122502 (2020)
- [4] Q. Ducasse, et al., Phys. Rev. C 94, 024614 (2016)
- [5] M. Sguazzin, et al., Phys. Rev. Lett. 134, 072501 (2025)
- [6] M. Sguazzin, et al., Phys. Rev. C 111, 024614 (2025)
- [7] K.-H. Schmidt, B. Jurado, Ch. Amouroux, C. Schmitt, Nuclear Data Sheets 131 (2016) 107-221